UCRL-CONF-204854

LAWRENCE
LIVERMORE
NATIONAL
LABORATORY

Turbulence Kinetic Energy Budgets and Dissipation Rates in Disturbed Stable Boundary Layers

J. K. Lundquist, M. Piper, B. Kosovic

June 23, 2004

16th Symposium on Boundary Layers and Turbulence
Portland, ME, United States
August 9, 2004 through August 13, 2004

Disclaimer

This document was prepared as an account of work sponsored by an agency of the United States Government. Neither the United States Government nor the University of California nor any of their employees, makes any warranty, express or implied, or assumes any legal liability or responsibility for the accuracy, completeness, or usefulness of any information, apparatus, product, or process disclosed, or represents that its use would not infringe privately owned rights. Reference herein to any specific commercial product, process, or service by trade name, trademark, manufacturer, or otherwise, does not necessarily constitute or imply its endorsement, recommendation, or favoring by the United States Government or the University of California. The views and opinions of authors expressed herein do not necessarily state or reflect those of the United States Government or the University of California, and shall not be used for advertising or product endorsement purposes.

4.9 TURBULENCE KINETIC ENERGY BUDGETS AND DISSIPATION RATES IN DISTURBED STABLE BOUNDARY LAYERS

Julie K. Lundquist*[1], Mark Piper[2], and Branko Kosović[1]

[1]Atmospheric Science Division
Lawrence Livermore National Laboratory, Livermore, CA, 94550

[2]Program in Atmospheric and Oceanic Science, University of Colorado at Boulder

1. INTRODUCTION

An important parameter in the numerical simulation of atmospheric boundary layers is the dissipation length scale, l_ε. It is especially important in weakly to moderately stable conditions, in which a tenuous balance between shear production of turbulence, buoyant destruction of turbulence, and turbulent dissipation is maintained. In large-scale models, the dissipation rate is often parameterized using a diagnostic equation based on the production of turbulent kinetic energy (TKE) and an estimate of the dissipation length scale. Proper parameterization of the dissipation length scale from experimental data requires accurate estimation of the rate of dissipation of TKE from experimental data.

Using data from the MICROFRONTS and CASES-99 field programs, we evaluate turbulent kinetic energy (TKE), TKE dissipation rate ε, and dissipation length l_ε over a range of stability regimes represented by a stable boundary layer (SBL), a destabilizing intrusion (by first a cold front and second a density current) and recovery. These data may be utilized to test recent parameterizations of dissipation rate ε and l_ε in order to determine the suitability of these models for inclusion in mesoscale models for numerical weather prediction or pollution dispersion prediction.

2. DATA SOURCES

Data from the MICROFRONTS and CASES-99 field programs are used in this study. The data from each experiment are described in the subsections below.

2.1 *MICROFRONTS (The cold front)*

The MICROFRONTS field experiment was conducted from 1 March 1995 through 30 March 1995 at a site approximately 75~km northeast of Wichita, near De Graff, Kansas. The field site was situated in gently rolling farmland in eastern Kansas, with a homogeneous fetch to the northwest. The ASTER facility, operated by the National Center for Atmospheric Research (NCAR) Atmospheric Technology Division, was deployed to collect turbulence data. The ASTER sonic anemometers were used to compute turbulence statistics for the three velocity components and used to estimate dissipation rate.

A dry Arctic cold front passed the MICROFRONTS site at approximately 0237 UTC (2037 LST) 20 March 1995, two hours after local sunset at 1839 LST. Time series spanning the period 0000-0600 UTC are shown in Figure 1.The 6-hr time period was chosen because it allows time for the front to completely pass the instrumented tower, with time on either side to view the state of the surface layer. The top two panels show wind speed and wind direction from the 10m south tower sonic anemometer, at a rate of 10 samples s^{-1}. The next panel shows dry bulb temperature from the 10m south tower platinum resistance thermometer, also at 10 samples s^{-1}. The last panel shows two surface layer scaling parameters, the local friction velocity $u*$ and the Monin-Obukhov scaling parameter $\zeta = z/L$, where L is a local Obukhov length. Both $u*$ and ζ are calculated from fluxes from the sonic anemometer at the 3m level. These scaling parameters are calculated using 900-s averaging intervals, centered on the time of the frontal passage. The dotted lines in Figure 1 delimit the frontal zone.

Note, visually, the sharp increase in wind speed variance with the passing of the front. After the front passes, the wind speed and speed variance decay to near prefrontal values. The wind has a southwesterly component in the prefrontal period. The temperature trace in panel 3 shows that there was a 2^oC rise in temperature starting at 0200 UTC, possibly due to advection of warmer air from the southwest or increased mixing in the surface layer. After the frontal passage, temperature decreased steadily due to radiational cooling and cold air advection. The wind shift and temperature drop were not coincident in this front, with the

temperature drop at 10m lagging the wind shift by about 180s. This is also observed in Taylor et al. (1993) and Shapiro et al. (1985), suggesting that this front may have an elevated head, like a density current.

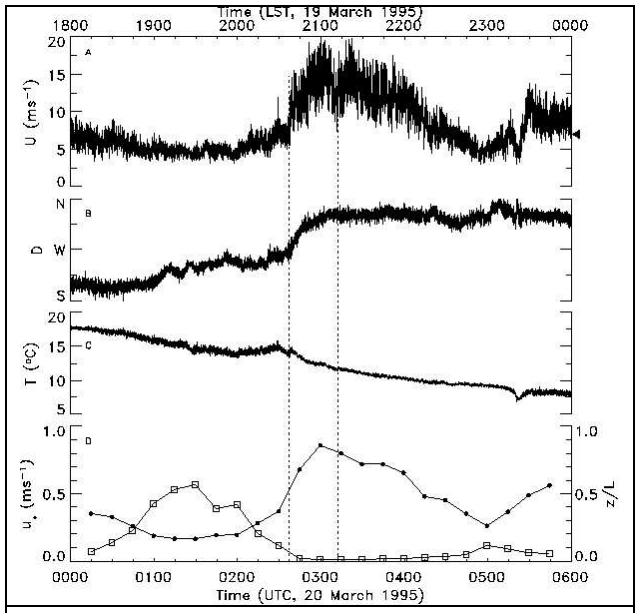

Figure 1: Time series from the 10m south tower instruments on 20 Mar 1995. (A) Wind speed from the sonic anemometer. (B) Wind direction from the sonic anemometer. (C) Temperature from the platinum resistance thermometer. (D) The friction velocity $u*$ (**.**) and the Monin-Obukhov scaling parameter ζ (squares). The dotted lines give the extent of the frontal zone.

2.2 *CASES-99: the density current*

The CASES-99 field experiment was conducted from 1 October 1999 through 30 October 1999 east of Wichita, near Leon, Kansas. An extensive array of instrumentation including a 60m tower, the HRDL lidar, boundary-layer wind profilers, radiosondes, a tethered lifting system, and two aircraft probed the nocturnal boundary layer throughout the field program (Poulos et al. 2002a). Local orographic relief did not exceed 30m, and yet several density currents were observed during early evenings throughout the field campaign.

A density current passed the CASES-99 main tower at approximately 0215 UTC (2115 LDT) 20 October 1999, two hours after local sunset at 1900 CDT and four hours after surface heat flux became negative. Figure 2 shows an 10 hour time series of wind speed, wind direction, virtual temperature T_v, $u*$, and heat flux from the sonic anemometer located at the 10m level. In addition to the 0215 UTC initial passage of the density current, another mixing event occurs at 0315 UTC. The later event is not accompanied by cooling and likely indicates the tail end of the density current. The top two panels show wind speed and wind direction at a rate of 10 samples sec^{-1}. The next panel shows virtual temperature measured by the sonic anemometer, also at 10 samples sec^{-1}. The bottom panel shows the friction velocity $u*$ and heat flux, also calculated with sonic anemometer data. The fluxes are calculated as covariances of perturbations from 720s mean values.

The 0215 UTC density current caused temperatures at 10m to drop from 10° to 6° C for a period of about five minutes. This pool of cooler air was confined to the region between the surface and 20m; higher levels (not shown) exhibited gradual cooling rather than an impulse of cold air. While the cold front was accompanied by a sharp increase in wind speed, the density current suppressed winds: wind speed decreases almost to zero momentarily, and the variance of wind speed is reduced following the passage of the density current. The passage of the density current is accompanied by an uplift-downdraft couplet (Blumen et al. 1999), as evident in the local maxima of heat flux.

The vertical lines on Figure 2 mark the beginning and the end of the density current as defined by the temperature decrease and concurrent wind shift at the 5m level. The 10m data, presented here, lag the 5m data, indicating that the head of the density current is tilted. This tilted structure is also evident in time-height cross sections of temperature, as shown in Poulos et al. (2002b).

3. DISSIPATION RATE CALCULATIONS

As described, for example, in Champagne et al. (1977), if $S_{u_i}(f)$ is the frequency spectrum of velocity component u_i in the inertial range and α_i is the Kolmogorov constant for the velocity component, the dissipation rate is given by

$$\varepsilon = \frac{2\pi}{U}\left(\frac{f^{5/3}S_{u_i}(f)}{\alpha_i}\right)^{3/2} .$$

This technique can be used by any high-frequency sensor that can measure velocities in the inertial range (Oncley et al. 1996). This method is compared with other methods of estimating ε during the MICROFRONTS experiment in paper 7.5 ("Surface-layer turbulence during a frontal passage," by Piper and Lundquist) of this volume and in Piper and Lundquist (2004). Only the

streamwise component is used for the calculations shown here. Values of ε are calculated in 300s intervals, whereas 60s intervals are presented in Piper and Lundquist (2004). The longer time series both smooths out small-scale fluctuations and increases the confidence in the calculations (Piper, 2001).

Figure 3 shows a time series of dissipation rate at 10m calculated for the 6 hour interval depicted in Figure 1. At the time of the frontal passage, dissipation rates increase to a maximum value of ~0.4 m^2s^{-3}, compared to prefrontal values of ~0.05 m^2s^{-3}. Dissipation rate levels remain high even after the passage of the frontal zone. Note that the maximum value here, at 10m height using 300s intervals, is one-third of the maximum value calculated using data from 3m height at 60s intervals, presented in Piper & Lundquist (2004). The increased dissipation rate in the frontal zone reflects the increased production of TKE due to mixing in the frontal zone.

Previous work (Blumen et al. 1999) has suggested that the head of a density current also induces turbulent mixing. Figure 4 depicts a time series of dissipation rate at 10m calculated for the 10 hour interval presented in Figure 2. Pre-density current values are ~ 0.1 m^2s^{-3}, twice those observed before the frontal passage in MICROFRONTS. Even more striking, the passage of the density current head is not marked by increased dissipation, as seen in Blumen et al. (1999), and would be expected from the peak in momentum and heat flux seen in Figure 2, but rather by a suppression of dissipation. Dissipation rates are less than 0.01 m^2s^{-3} from the time of the passage of the head through until its end. This unique response could be a function of the relatively long interval (300s) used for calculating ε compared to the time required for the head of the density current to pass; this behavior will be investigated in future work.

4. COMPARISONS OF OBSERVED DISSIPATION LENGTH WITH PROPOSED MODELS

The calculations presented above, as well as those from different levels during the same time periods will be compared with several proposed models for dissipation length. Dissipation length l_ε is typically proposed to be a related to local stability, either through a gradient Richardson number, a flux Richardson number, or a local Froude number. The parameterizations offered by Cheng & Canuto (1994) and Freedman and Jacobson (2003) will be considered.

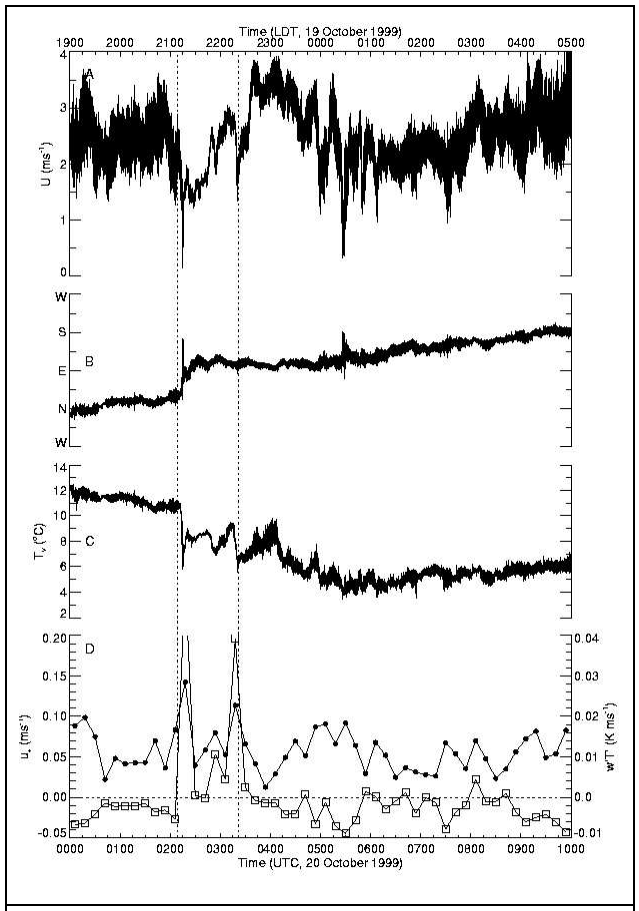

Figure 2: Time series from the sonic anemometer mounted at 10m on the main 60m CASES-99 tower on 20 Oct 1999. (A) Wind speed. (B) Wind direction. (C) Virtual temperature. (D) Friction velocity $u*$ and heat flux wT'. Dotted lines mark the passage of the density current as defined by the temperature shift at the 5m level; note that the 10m level (shown here) slightly lags the 5m level, indicating a tilted structure to the head of the density current.

5. SUMMARY

Observations of turbulent kinetic energy dissipation rate in disturbed stable boundary layers exhibit great variability. In the 20 March 1995 frontal passage, the dissipation rate is found to increase by nearly an order of magnitude to a maximum value of ~0.4 m^2s^{-3}, compared to prefrontal values of ~0.05 m^2s^{-3}. Dissipation rate levels remain high even after the passage of the frontal zone. In the 20 October 1999 density current, the density current suppresses TKE dissipation, from pre-density current values ~ 0.1 m^2s^{-3} to less than 0.01 m^2s^{-3}. The broad range of

stability conditions offered by these two cases creates an ideal testbed for parameterizations of TKE dissipation and TKE dissipation length l_ε.

Acknowledgements

Support for MP has been provided by the Air Force Office of Scientific Research under Grant F49620-95-1-014-1 and under AASERT Grant F49620-97-1-0448. Support for MP and JKL at the University of Colorado has been provided by the Atmospheric Sciences Division, Mesoscale Dynamcis Program of the National Science Foundation under Grant ATM-9903645. MP also thanks Research Systems, Inc. for allowing a leave of absence. This work was performed under the auspices of the U.S. Department of Energy by the University of California, Lawrence Livermore National Laboratory under contract No. W-7405-Eng-48.

References

Blumen, W., R.L. Grossman, and M. Piper, 1999: Analysis of heat budget, dissipation and frontogenesis in a shallow density current. *Bound.-Layer Meteorol.*, **91**, 281-306.

Champagne, F.H., C.A. Friehe, J.C. LaRue, and J.C. Wyngaard, 1977: Flux measurements, flux estimation techniques, and fine-scale turbulence measurements in the unstable surface layer over land. *J. Atmos. Sci.*, **34**, 515-530.

Cheng, Y. and V.M. Canuto, 1994: Stably stratified shear turbulence: A new model for the energy dissipation length scale. *J. Atmos. Sci.*, **51**, 2384-2396.

Freedman, F. R. and M. Z. Jacobson. 2003: Modification of the standard ε-equation for the stable ABL through enforced consistency with Monin-Obukhov similarity theory. *Bound.-Layer Meteorol.*, **106**, 383-410.

Oncley, S.P., C.A. Friehe, J.A. Businger, E.C. Itsweire, J. C. LaRue and S.S. Chang, 1996: Surface-layer fluxes, profiles, and turbulence measurements over uniform terrain under near-neutral conditions. *J. Atmos. Sci.*, **53**, 1029-1044.

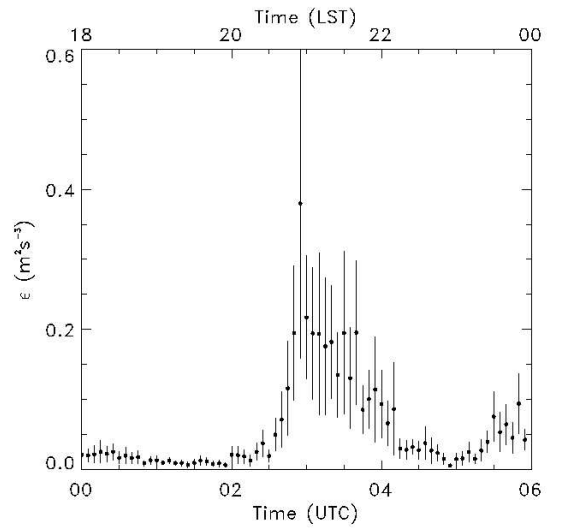

Figure 3: Inertial dissipation rate calculations from the 10m sonic anemometer for the 20 Mar 1995 front. Values of ε are calculated in 300s intervals. Error bars denote 95% confidence intervals on the means.

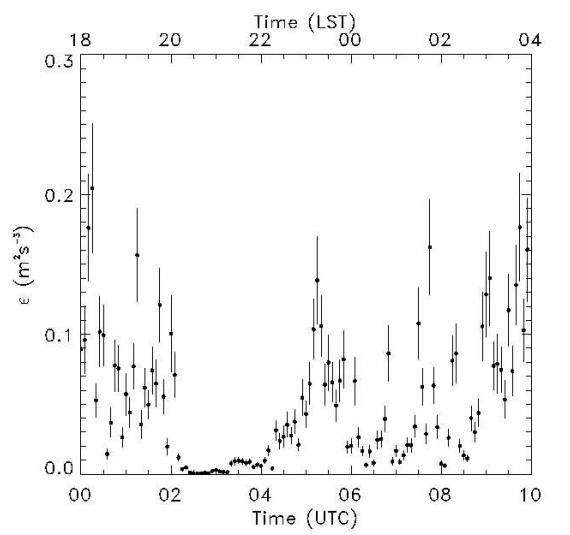

Figure 4:. Inertial dissipation rate calculations from the 10m sonic anemometer for the 20 Oct 1999 density current. Values of ε are calculated in 300s intervals. Error bars denote 95% confidence intervals on the means. Note the expanded ordinate, in comparison to that in Figure 3.

Piper, M., 2001: The Effects of a Frontal Passage on Fine-Scale Nocturnal Boundary Layer Turbulence. Ph.D. dissertation, University of Colorado at Boulder, Dept. of Astrophysical, Planetary, and Atmospheric Sciences, 217 pp.

Piper, M., and J. K. Lundquist, 2004: Surface-Layer Turbulence Measurements during a Frontal Passage. *J. Atmos. Sci.*, to appear.

Poulos, G.S., and co-authors, 2002a: CASES-99: A comprehensive investigation of the stable nocturnal boundary layer. *Bull. Amer. Meteor. Soc.*, **83**, 555-581.

Poulos, G.S., J.K. Lundquist, W. Blumen, and S. Neuville, 2002b: Shallow Slope Density Currents during CASES-99: Observations and Modeling. *15th Symposium on Boundary Layers and Turbulence*, Wageningen, The Netherlands, pp. 481-484.